Accepted Manuscript

Magnetic ethyl-based organosilica supported Schiff-base/indium: A very efficient and highly durable nanocatalyst

Reza Mirbagheri, Dawood Elhamifar

PII: S0925-8388(19)31019-9

DOI: https://doi.org/10.1016/j.jallcom.2019.03.203

Reference: JALCOM 49967

To appear in: *Journal of Alloys and Compounds*

Received Date: 1 February 2019

Revised Date: 4 March 2019

Accepted Date: 13 March 2019

Please cite this article as: R. Mirbagheri, D. Elhamifar, Magnetic ethyl-based organosilica supported Schiff-base/indium: A very efficient and highly durable nanocatalyst, *Journal of Alloys and Compounds* (2019), doi: https://doi.org/10.1016/j.jallcom.2019.03.203.

Graphical abstract

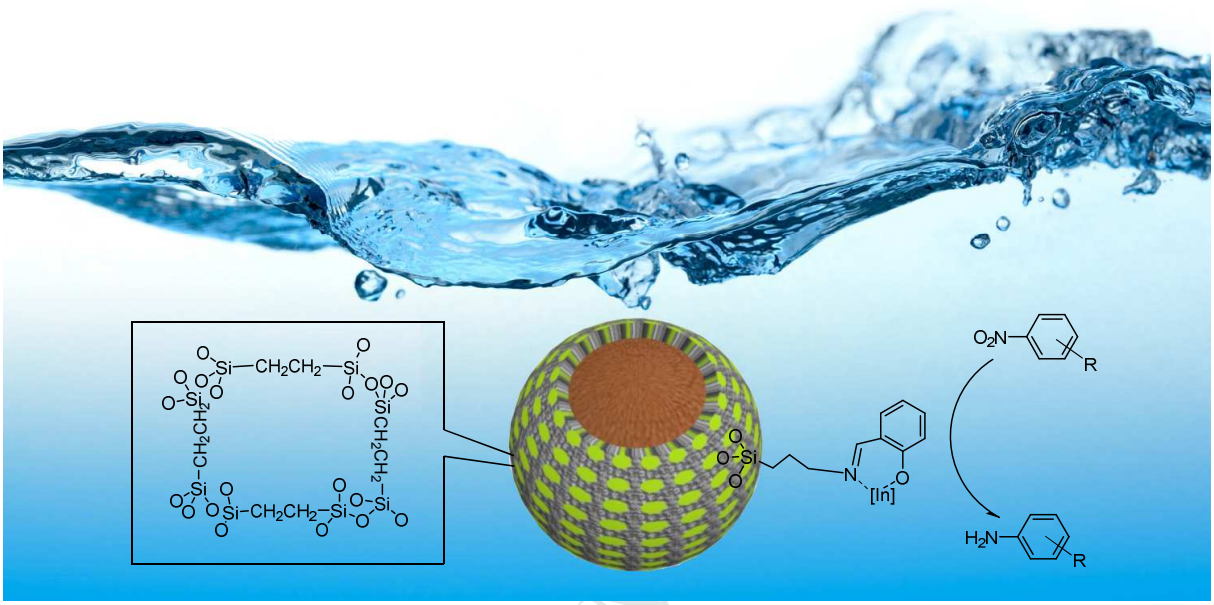

Magnetic ethyl-based organosilica supported Schiff-base/indium: A very efficient and highly durable nanocatalyst

Reza Mirbagheri and Dawood Elhamifar*

Department of Chemistry, Yasouj University Yasouj 75918-74831, Iran

E-mail: d.elhamifar@yu.ac.ir

Abstract

In the present study a novel core-shell structured magnetic bifunctional organosilica was prepared through modification of Fe_3O_4 nanoparticles with a mixture of bis(triethoxysilyl) ethane (BTES) and 3-aminopropyltrimethoxysilane (APTES) followed by treatment with 2-hydroxybenzaldehyde. This nanomaterial was applied as efficient support for immobilization of indium chloride. The prepared nanomaterial was denoted as Fe_3O_4@BOS@SB/In and characterized using Fourier transform infrared (FT-IR) spectroscopy, thermal gravimetric analysis (TGA), energy-dispersive X-ray (EDX) spectroscopy, scanning electron microscopy (SEM), transmission electron microscopy (TEM), vibrating sample magnetometer (VSM) and powder X-ray diffraction (PXRD). The Fe_3O_4@BOS@SB/In was successfully applied as a powerful catalyst for green reduction of nitobenzenes in water at room temperature. This catalyst was recovered and reused several times without significant decrease in efficiency and stability.

Keywords: Magnetic nanoparticles, Core-shell, Schiff-base, Indium nanocatalyst, Reduction of nitrobenzenes

1. Introduction

Magnetic iron oxides are one of the most important nanoparticles between chemists that have been successfully used in different fields such as computer [1, 2],_electronics [3-5], health [6-9], medicine [10-14] and even in our daily life [15, 16]. Also in chemistry, the use of magnetic energy is very significant because its environmentally-friendly, low cast and so beneficial in catalytic processes [17-21]. In the field of nanochemistry, also the aforementioned MNs are so popular and there are many reports in this area [22-24]. Especially Fe_3O_4 NPs are widely used in many catalytic reactions due to their easy preparation, controllable particle size and also low cast. Despite these advantages, the Fe_3O_4 nanoparticles suffer from some restrictions such as high surface energy and instability in the presence of air and acidic media [25, 26]. To overcome these limitations, these MNs are modified with suitable stabilizers such as carbon [27, 28], silica [29, 30] and polymer [31-33]. Among these, silica based ones is more interested due to high stability, eco-friendly, non-toxicity as well as excellent capacity and surface area for immobilization and stabilization of catalytic species [10, 34-37]. However, it is more desirable to modify the Fe_3O_4@SiO_2 surface with organic functional groups to increase the lipophilicity of the silica shells for catalytic organic reactions. The modification of magnetic silicas with organic moieties is achieved through both grafting and sol-gel approaches. To date some magnetic organosilicas have been prepared and applied in catalysis and adsorption processes [38-40]. Some of recently developed systems are MNPs with 1,3-bis(4-triethoxysilyl-2,6-diisopropylphenyl)-imiadzol-3-ium-trifluoro-methane (NHC) bridged groups supported palladium used as catalyst for the Suzuki–Miyaura coupling [40], proline-functionalized MNP used as efficient and recyclable catalyst for aldol condensation [41], magnetically separable 2D-hexagonally ordered thiol functionalized mesoporous silica material (Fe@TFMS) applied as

catalyst in the biodiesel production [42], Fe_3O_4@mesoporous SBA-15 used as a robust and magnetically recoverable catalyst for Biginelli reaction [43] and magnetic nanoparticles supported Schiff-base/copper complex used as a nanocatalyst for preparation of 3,4-dihydropyrimidinones [37]. Other interesting magnetic organosilicas were also prepared and applied in a number of chemical processes [40, 44-46].

On the other hand, one of the most important transformations in chemistry is reduction of organic compounds that has wide applications in chemical synthesis and industries such as pulp and paper [47], pharmaceutical [48], metal recovery [49] and textiles [50]. Especially, reduction of nitrobenzenes is more attracted due to the corresponding anilines are valuable intermediate in different areas such as drug synthesis, rubber processing chemicals, dyes and pigments [51]. The use of a metal as catalyst in the presence of reducing agents is a common method for reduction of nitro-compounds [52]. Some of recently developed catalytic systems are Fe/ hydrazine [53], Au/H_2 [54], Ag/$NaBH_4$ [55], Pd@NA@GO/$NaBH_4$ [56], Pd–Fe_3O_4–Sm_2O_3–ZrO_2/$NaBH_4$ [57] and Pt-Ni catalyst/$NaBH_4$ [58]. In addition, several indium-based catalysts have been reported in this matter [59, 60]. However, most of these indium based catalysts have been applied under homogeneous conditions in a toxic organic solvent and suffer from disadvantages such as difficulty in and product separation, catalyst recovery and environmental pollution. Consequently, there is a need to design and prepare suitable heterogeneous catalysts with high efficiency and recoverability for reduction of nitrobenzenes. According to these notes and also due to importance of magnetic-organosilica nanoparticles in catalysis chemistry, in the present study we have designed novel magnetic bi-functional organosilica nanoparticles supported Schiff-base/indium complex (Fe_3O_4@BOS@SB/In) with improved catalytic activity and reusability in the green reduction of nitrobenzenes (Scheme 1). The Fe_3O_4@BOS@SB/In was

prepared and completely characterized using various techniques such as Fourier transform infrared (FT-IR) spectroscopy, thermal gravimetric analysis (TGA), energy-dispersive X-ray spectroscopy (EDS), scanning electron microscopy (SEM), vibrating sample magnetometer (VSM), transmission electron microscopy (TEM) and powder X-ray diffraction (PXRD).

2. Experimental section

All materials were used as received without further purification. $FeCl_2.4H_2O$ and $FeCl_3.6H_2O$ (Merck, 99%), 1,2-bis(triethoxysilyl)ethane (BTEE) (Aldrich, 96%), (3-aminopropyl)triethoxysilane (APTES) (Aldrich, 98%), salicylaldehyde (Merck, 99%), indium(III) chloride (Aldrich, 98%) were purchased and used in this study. Solvents were dried and purified before use according to standard procedures. Scanning electron microscopy (SEM) analysis was performed on a Philips, XL30 emission electron microscope. The thermal gravimetric analysis (TGA) was measured from room temperature to 800 °C by NETZSCH STA 409 PC/PG. Fourier transform infrared (FT-IR) spectroscopy was recorded on a Brucker-Vector 22 spectrometer. Energy dispersive X-ray spectroscopy (EDX) was carried out by TESCAN Vega Model. Powder X-ray diffraction (PXRD) was obtained using a Panalytical X-Pert diffractometer. Transmission electron microscopy (TEM) images were taken on a FEI TECNAI 12 BioTWIN microscope.

2.1. Preparation of Fe_3O_4 nanoparticles supported bifunctional organosilica (Fe_3O_4@BOS)

For this purpose, at first Fe_3O_4 nanoparticles were synthesized according to a well-known procedure using 2 g of $FeCl_2.4H_2O$, 3 g of $FeCl_3.6H_2O$ in H_2O (25 mL) and ammonia (40 mL, 25 %) [61]. Then, Fe_3O_4@BOS was prepared *via* a sol-gel method. For this, 0.5 g of Fe_3O_4

nanoparticles were completely dispersed in solution of deionized water (6 mL) and ethanol (22.5 mL) under argon atmosphere. Then 3-aminopropyltrimethoxysilane (APTES, 0.5 mL), 1,2-bis(triethoxysilyl)ethane (BTEE, 1 mL) and ammonia (2 mL, 25 %) were slowly added in reaction vessel while stirring vigorously. After 16 hours, the resulting product was collected using an external magnetic field and completely washed with a mixture of water and ethanol. Finally, this material was dried at 60 °C for 12 h and denoted as Fe_3O_4@BOS.

2.2. Preparation of the Fe_3O_4@BOS@SB material with core-shell structure

For preparation of Fe_3O_4 nanoparticles supported bifunctional organosilica with Schiff base group (Fe_3O_4@BOS@SB), 0.5 g of Fe_3O_4@BOS was firstly dispersed in toluene (10 mL) for 10 min. Then, 2-hydroxybenzaldehyde (2 mL) was added and the obtained mixture was refluxed under argon atmosphere for 24 h. The resulting material was collected using an external magnet, washed completely with EtOH, dried at 60 °C for 12 h and denoted as Fe_3O_4@BOS@SB.

2.3.Preparation of the Fe_3O_4@BOS@SB supported indium (Fe_3O_4@BOS@SB/In)

For immobilization of indium, Fe_3O_4@BOS@SB (0.5 g) was firstly dispersed in acetonitrile for 10 min. Then, $InCl_3$ (0.5 g) was added into reaction vessel and this mixture was stirred at room temperature for 48 h under argon atmosphere. The resulting material was collected using an external magnetic field, washed completely with acetonitrile, dried at 60 °C for 12 h and denoted as Fe_3O_4@BOS@SB/In. According to EDS analysis the loading of indium amount on material surface was obtained to be 0.5 mmol/g.

2.4.General procedure for the reduction of nitrobenzenes using Fe_3O_4@BOS@SB/In catalyst

In a typical procedure, 1 mmol of nitrobenzene, 2 mmol of sodium borohydride and 0.5 mol% of the Fe_3O_4@BOS@SB/In catalyst were added in water. This mixture was stirred at room temperature and progress of the reaction was monitored by TLC. After finishing of the reaction, the catalyst was removed using a magnetic field and the aniline product was obtained by cooling the residue mixture in an ice bath and then filtering.

2.5.General procedure for the recovery of Fe_3O_4@BOS@SB/In nanocatalyst

For this, 4-nitrobenzaldehyde (1 mmol), $NaBH_4$ (2 mmol) and Fe_3O_4@BOS@SB/In (0.5 mol%) were added in water. The resulted mixture was magnetically stirred at room temperature. After completion of the reaction, the catalyst was separated using an external magnet and the product was obtained as previous procedure. The recovered catalyst was dried and applied in the next run under the same conditions as the first run. These steps were repeated several times and the yield of each run was calculated.

2.6. General procedure for the leaching test on Fe_3O_4@BOS@SB/In nanocatalyst

For this, 4-nitrobenzaldehyde (1 mmol), $NaBH_4$ (2 mmol) and Fe_3O_4@BOS@SB/In (0.5 mol%) were added in water (5 mL). After 5 minutes mixing, the catalyst was separated by an external magnetic field and the catalyst-free mixture was allowed to stir for 20 minutes under optimized conditions. The progress of the reaction was monitored by TLC.

3. Results and discussion

For the preparation of the desired catalyst, firstly the magnetic bifunctional organosilica (Fe_3O_4@BOS) was prepared *via* hydrolysis and co-condensation of 1,2-bis(triethoxysilyl)ethane (BTEE) and 3-aminopropyltriethoxysilane (APTES) around Fe_3O_4 nanoparticles. This was then

modified with 2-hydroxybenzaldehyde to deliver corresponding Schiff-base ligand (Fe_3O_4@BOS@SB). Finally, the Fe_3O_4@BOS@SB/In nanocatalyst was obtained through immobilization of $InCl_3$ onto Fe_3O_4@BOS@SB (Scheme 1). This catalyst was characterized using several techniques such as FT-IR, TGA, EDS, SEM, VSM, TEM and PXRD.

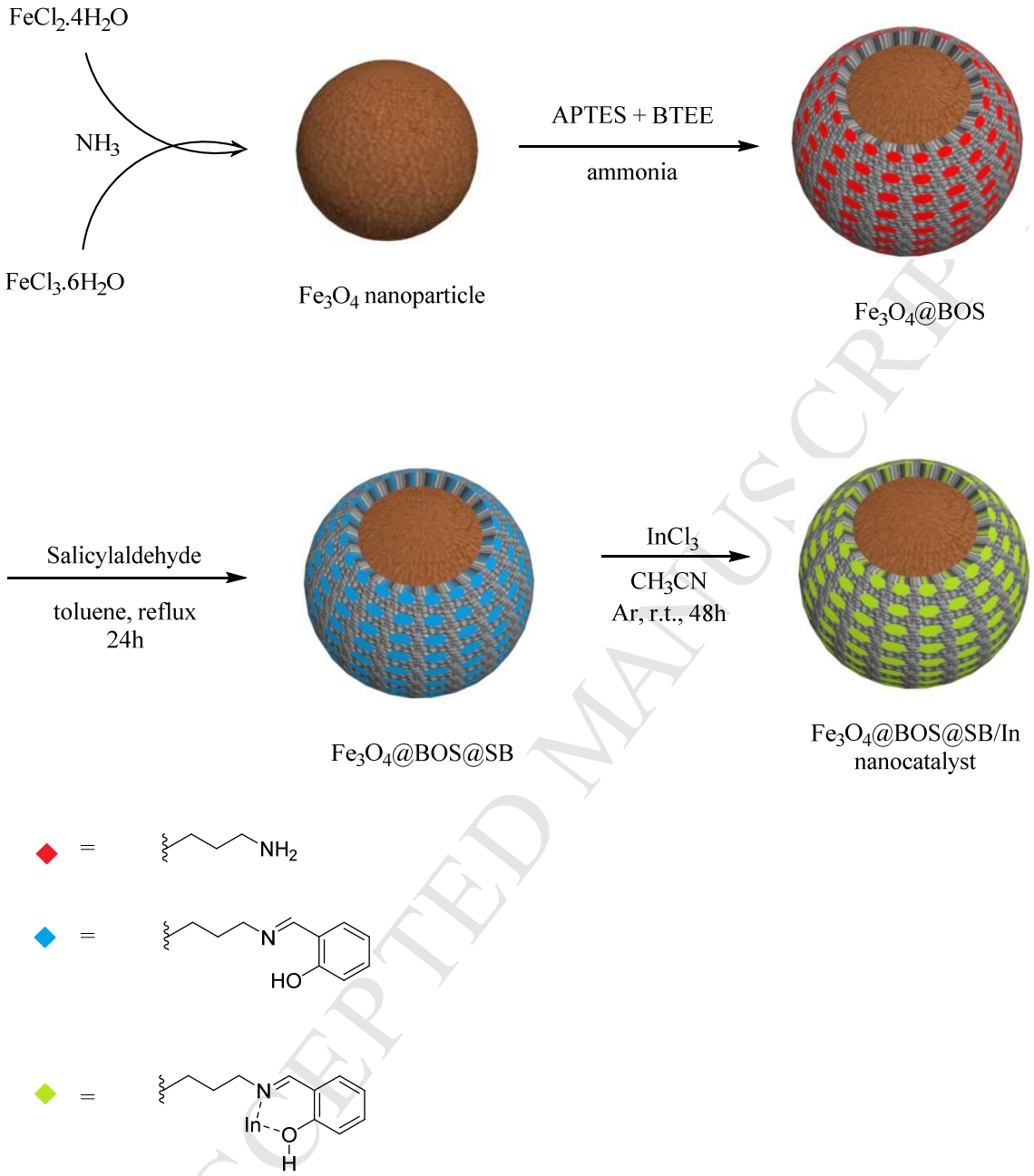

Scheme 1. Preparation of Fe_3O_4@BOS@SB/In nanocatalyst

The magnetic property of the catalyst was investigated using vibrating sample magnetometer (VSM) analysis (Figure 1). This showed a magnetic ability about 12.5 emu/g for the Fe_3O_4@BOS@SB/In that is lower than magnetic Fe_3O_4 NPs confirming successful modification of iron oxide cores with organosilica shells.

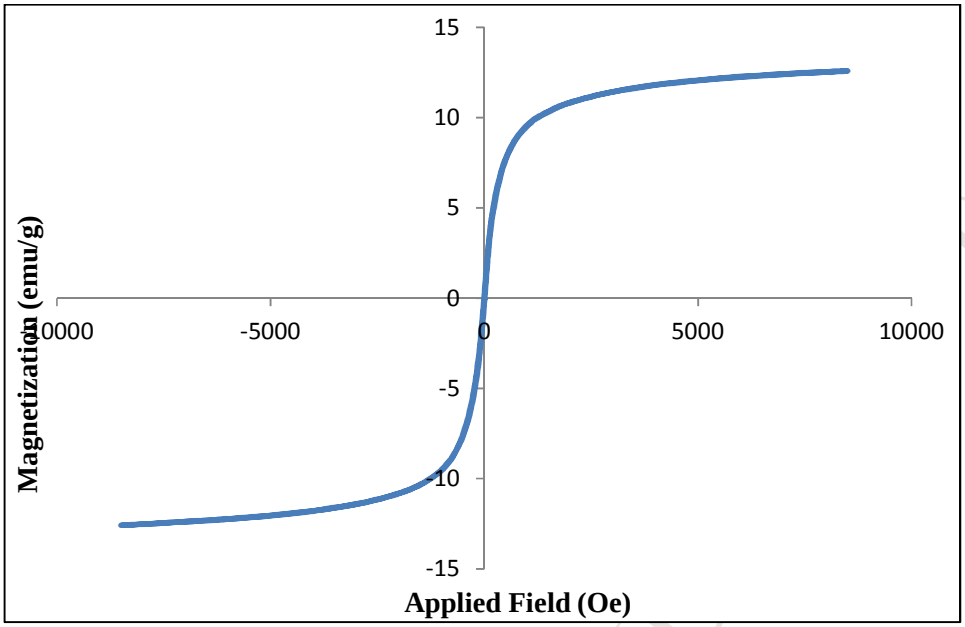

Figure 1. VSM pattern of Fe_3O_4@BOS@SB/In nanocatalyst

Thermal gravimetric (TG) analysis was performed to study the thermal stability of the material. As shown in Figure,2 a weight loss of about 2.5 % below 120 °C is due to removal of physically adsorbed water and organic solvents. Afterward, two weight losses were found, first one about 8 % at 200–400 °C and the second one about 18% at 401–800 °C corresponding to elimination of supported propyl-Schiff-base and incorporated bridged-ethyl groups, respectively. These confirm well-immobilization of ethyl and propyl-Schiff-base functional groups onto/into material framework and also show high thermal stability of the catalyst.

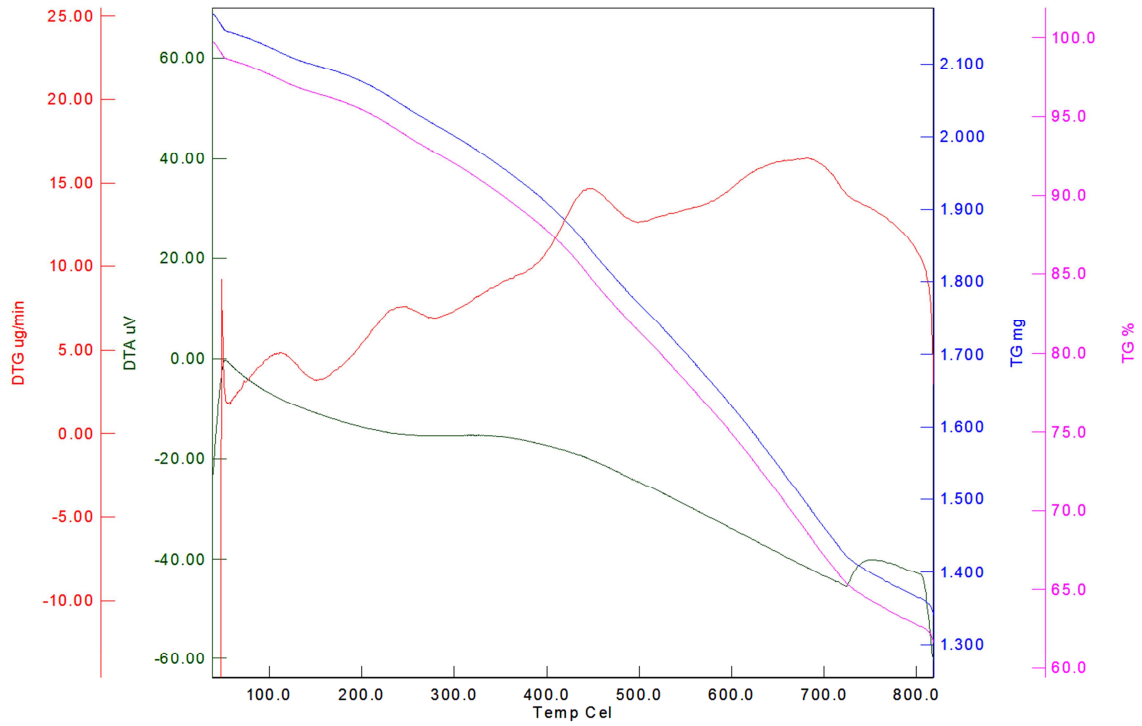

Figure 2. TG analysis of the Fe_3O_4@BOS@SB/In nanocatalyst

Energy-dispersive X-ray spectroscopy (EDS) demonstrated the presence of In, Fe, Si, C, N, O and Cl elements in the material proving successful incorporation and/or immobilization of organic groups and indium chloride into/onto material framework (Figure 3).

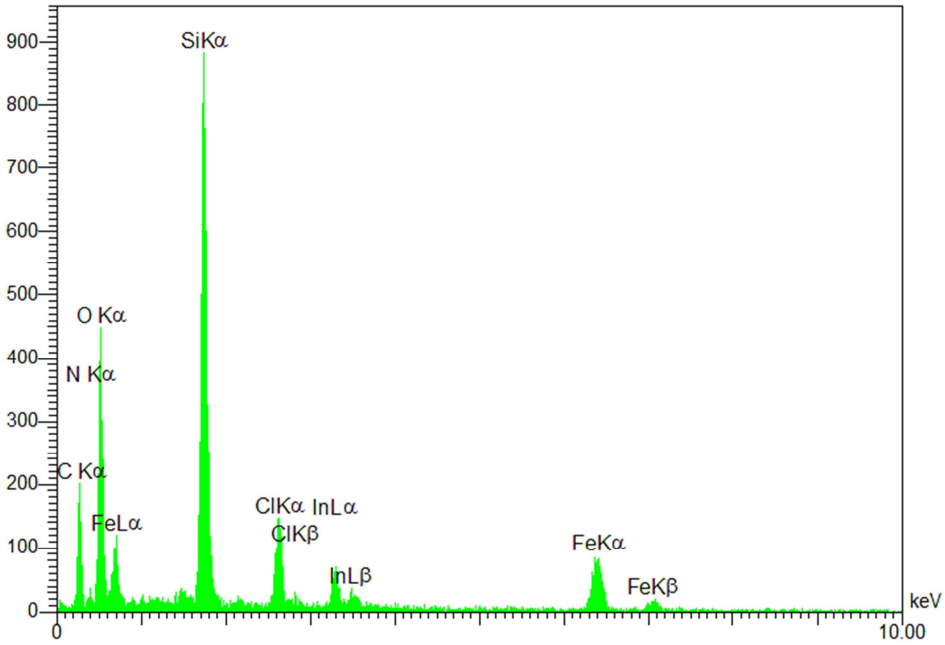

Figure 3. EDS spectrum of the Fe_3O_4@BOS@SB/In nanocatalyst

Fourier transform infrared (FT-IR) spectra of Fe_3O_4, Fe_3O_4@BOS, Fe_3O_4@BOS@SB and Fe_3O_4@BOS@SB/In are demonstrated in Figure 4. For all samples the signal of F-O bond is observed about 573 cm^{-1}. The absorption peaks at 700–800 cm^{-1} are attributed to C–Si stretching vibrations. The bands observed at 1095 and 930 cm^{-1} are assigned to the symmetric and asymmetric stretching vibrations of Si–O–Si bonds. C–H stretching vibrations of ethyl and propyl functional groups are observed at 2927 cm^{-1}. In addition, the broad signal around 3350 cm^{-1} can be assigned to N–H and O–H bonds of material surface. Interestingly, for Fe_3O_4@BOS@SB/In a new peak at 1645 cm^{-1} corresponding to C=N bond is observed confirming successful formation of Schiff-base ligand during catalyst preparation (Figure 4c, 4d). These are in good agreement with EDS and TGA results and successfully confirm the presence of expected functional groups in the structure of the material.

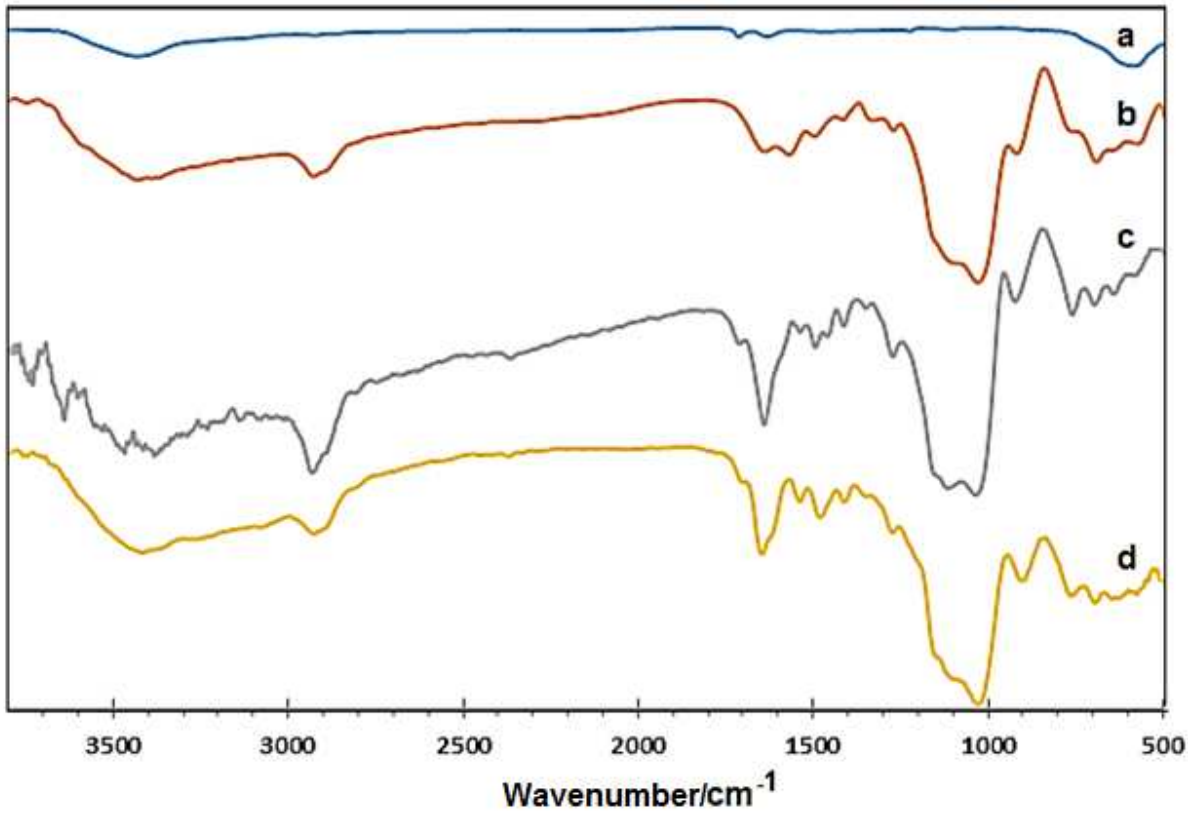

Figure 4. FT-IR spectra of the Fe_3O_4 (a), Fe_3O_4@BOS (b), Fe_3O_4@BOS@SB (c) and Fe_3O_4@BOS@SB/In (d)

The morphology and particle size of the catalyst was determined using SEM (Figure 5). This showed well-distributed spherical particles with average size of 50 nm. Moreover, the uniformity and well-ordering of the particles are also clear in this Figure.

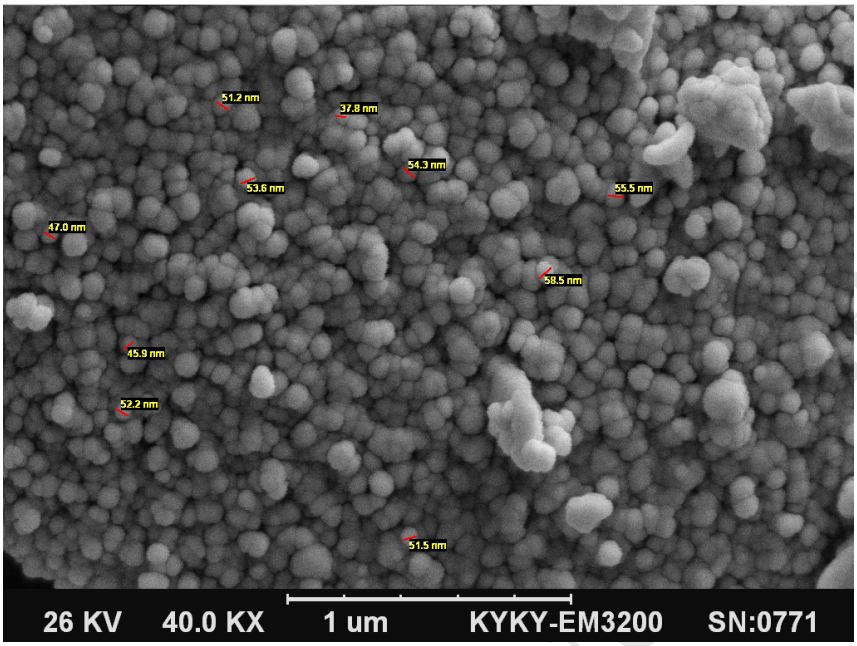

Figure 5. SEM image of the Fe_3O_4@BOS@SB/In nanocatalyst

According to TEM image (Figure 6) the designed nanocatalyst has a core-shell structure with black core (Fe_3O_4) and gray shell (organosilica).

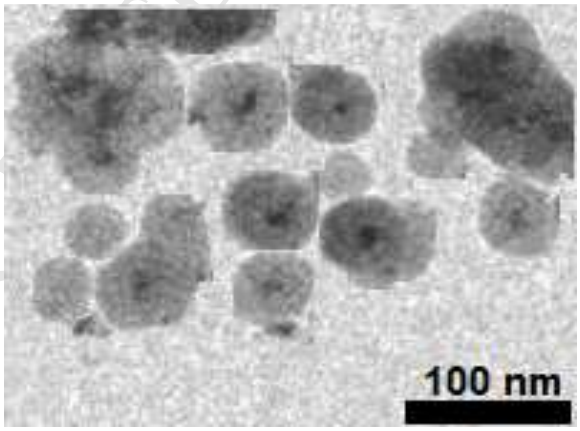

Figure 6. TEM image of the Fe_3O_4@BOS@SB/In nanocatalyst

The availability of Fe_3O_4 NPs in Fe_3O_4@BOS, Fe_3O_4@BOS@SB and Fe_3O_4@BOS@SB/In nanomaterials was determined by powder X-ray diffraction (PXRD) analysis (Figure 7).For all samples the Miller indices values (hkl) of 220, 311, 400, 422, 511 and 440 are cleared, respectively, at 2θ of 30, 36, 43, 54, 57 and 64 degrees. These prove good to high magnetic properties of designed materials. In fact, the aforementioned peaks are corresponded to Fe_3O_4 NPs and confirm high stability of crystalline structure of these particles during catalyst preparation. Moreover, the intensity of aforementioned peaks is decreased after each modification step confirming the successful incorporation and/or immobilization of organic and inorganic species onto magnetic iron oxide surface.

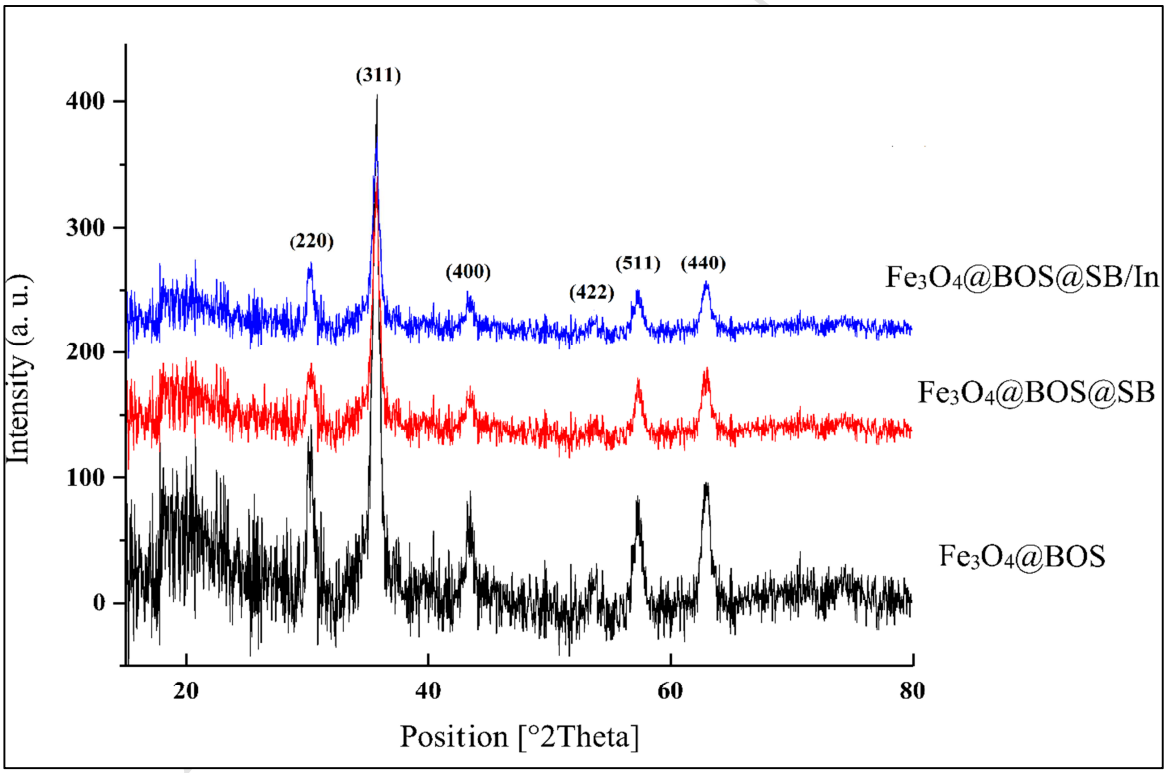

Figure 7. PXRD analysis of Fe_3O_4@BOS (black), Fe_3O_4@BOS@SB (red) and Fe_3O_4@BOS@SB/In nanocatalyst (blue)

After successful characterization, the catalytic efficiency of the designed Fe_3O_4@BOS@SB/In nanocatalyst was studied in the reduction of nitrobenzenes. Although there are some reports about reduction ability of $InCl_3$ under homogeneous conditions [62, 63], however, all of these studies suffer from the restrictions of product separation, catalyst recoverability and additional boring steps in extraction process. Therefore, the use of supported IN-catalyst is important subject in this matter. To test the activity of our indium-based catalyst, the reduction of 4-nitrobenzaldehyde was selected as a reaction model (Table 1). To obtain the optimum conditions, the effect of solvent and catalyst loading was investigated in the reaction progress. Various solvents such as ethanol, water, methanol and THF were tested (Table 1, entries 1-4). It is important to note that the use of a protic polar solvent will increase the reaction rate due to release H_2 in the presence of $NaBH_4$ [64]. As seen in Table 1, the catalyst efficiency is increased by changing solvent from ethanol and methanol to water. In THF a low yield is observed. This is due to formation of a borane/tetrahydrofuran complex (THF-BH_3) during applied conditions [60]. Then the amount of catalyst was optimized and the best result was obtained in the presence of 0.5 mol% of Fe_3O_4@BOS@SB/In nanocatalyst (Table 1, entries 4-6). To show the neat effect of indium centers in the catalytic process, the model reaction was performed without catalyst as well as in the presence of indium-free Fe_3O_4@BOS@SB and Fe_3O_4@BOS materials under conditions as above. Interestingly, for all of these no conversion was observed indicating that the reduction process is actually catalyzed by supported indium species (Table 1, entries 7-9).

Table 1 Optimization of the reaction conditions in reduction of 4-nitrobenzaldehyde

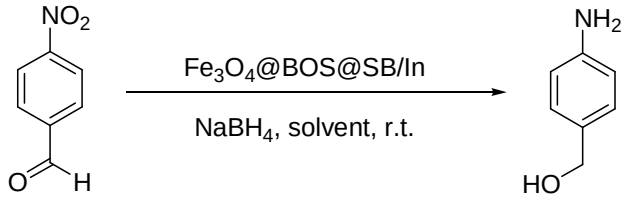

Entry	Catalyst (mol %)	Solvent	Time (min)	Yield (%)[b]
1	0.25	EtOH	12	20
2	0.25	MeOH	12	32
3	0.25	Water	12	53
4	0.25	THF	12	35
5	**0.5**	**Water**	**12**	**90**
6	0.7	Water	12	90
7	-	Water	12	-[c]
8	Fe_3O_4@BOS@SB [d]	Water	12	-[c]
9	Fe_3O_4@BOS [e]	Water	12	-[c]

[a] Reaction conditions: 4-nitrobenzaldehyde (1 mmol), $NaBH_4$ (2 mmol), room temperature. [b] Isolated yield. [c] No conversion was observed during reaction time. [d] 0.01 g of Fe_3O_4@BOS@SB was used. [e] 0.01 g of Fe_3O_4@BOS was used.

After optimization of the reaction conditions, various derivatives of nitrobenzene were used as substrate to investigate the activity of the catalyst (Table 2). Interestingly, both electron-withdrawing and electron-donating substituents containing nitrobenzens were successfully

converted to their corresponding aniline derivatives at room temperature and very short times. It is also important to note that the carbonyl functional moieties of substrates were also reduced to their corresponding alcohol adducts under applied conditions (Table 2, entry 3). These results strongly confirm high efficiency of designed nanocatalyst for green and fast reduction of different nitrobenzene derivatives at room temperature that is an excellent advantage in the green chemistry world.

Table 2. Reduction of nitrobenzenes using Fe_3O_4@BOS@SB/In nanocatalyst

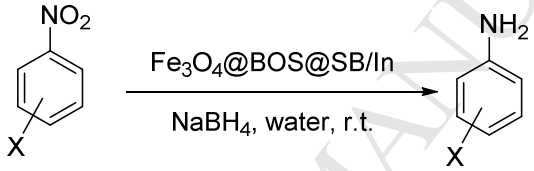

Entry	X	Product	Time (min)	Yield (%) [b]	M. P. (°C) Found	M. P. (°C) Reported [65]
1	4-Cl	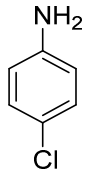	7	94	70-72	67-70
2	4-NH_2	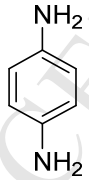	7	92	143-145	138-143
3	4-CHO	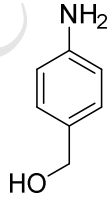	12	90	61-63	60-65

Table 2, continued

4	4-CH_2OH	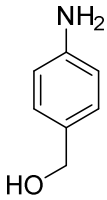	7	93	61-63	60-65
5	2-OH	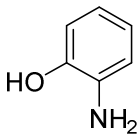	12	87	171-173	170-175
6	2-CH_2OH	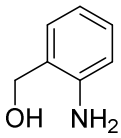	10	91	79-81	81-83

[a] Reaction conditions: Nitrobenzene derivative (1 mmol), $NaBH_4$ (2 mmol), catalyst (0.5 mol%), H_2O (3 mL) at room temperature. [b] Isolated yield

In the next, the recoverability and reusability of desired indium-based catalyst were studied (Figure 8). For this, after the reaction was completed, the catalyst was collected and separated using an external magnetic field and it was reused in the next run under applied conditions as the first run. These experiments were repeated and it was found that the catalyst could be recovered and reused at least 6 times with keeping its productivity (Figure 8).

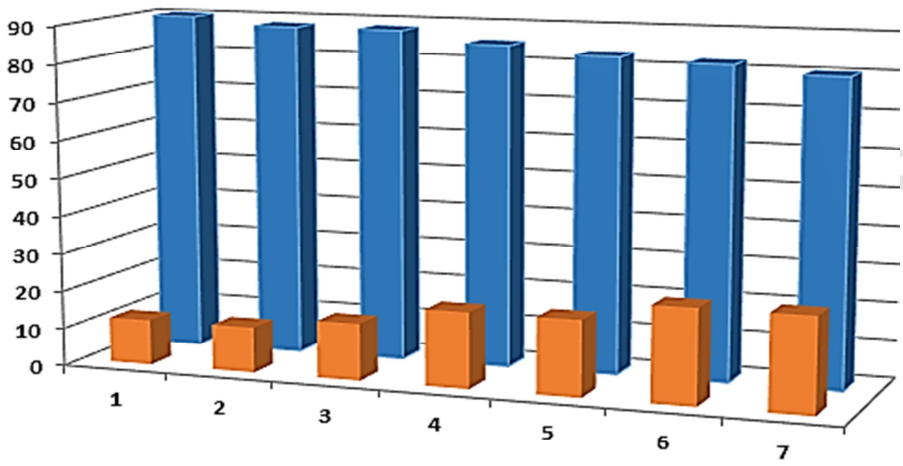

Run	1	2	3	4	5	6	7
Time (min)	12	12	15	20	20	25	25
Yield (%)	90	88	88	85	83	82	80

Figure 8. The reusability of Fe_3O_4@BOS@SB/In nanocatalyst

To show the nature of actual catalyst in the reaction process, in another study a leaching test was performed. To do this, after about 50% of the reduction process was completed, it was stopped and the catalyst was removed using an external magnet. The catalyst-free filtrate was then allowed to continue for 20 minutes. Pleasingly, in this case no further conversion was observed indicating that the catalyst operates in a heterogeneous manner. Also to verify chemical stability of the catalyst, the XRD analysis of the recovered nanocatalyst was performed. As shown in Figure 9, the pattern of Miller indices values (hkl) is the same as its parent confirming the high chemical stability of Fe_3O_4@BOS@SB/In nanocatalyst during applied conditions.

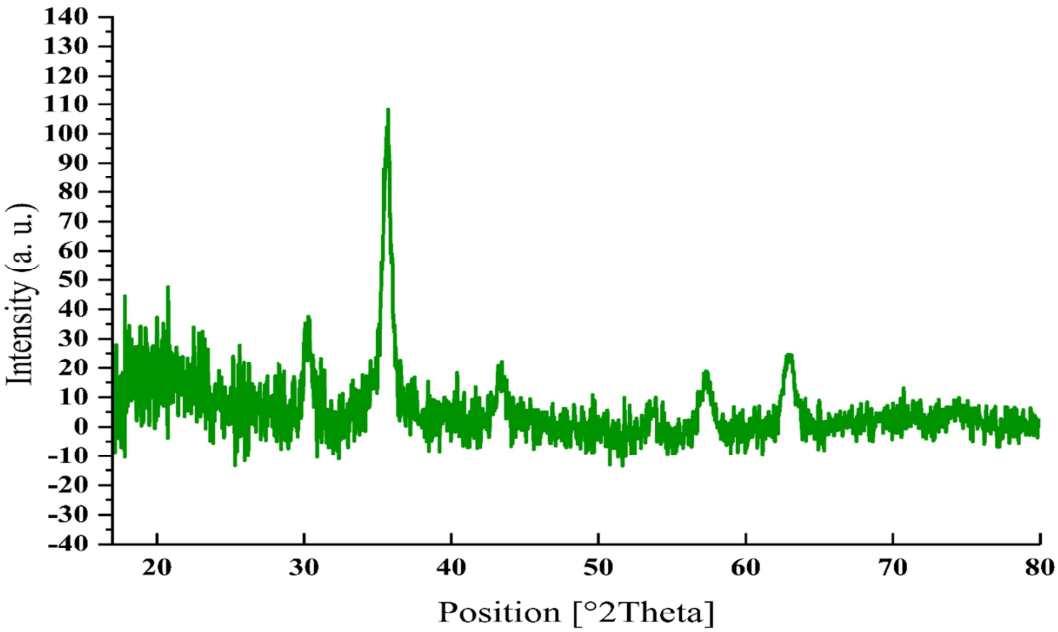

Figure 9. The XRD analysis of the recovered nanocatalyst after nitrobenzene reduction

In the final study, the performance of our catalyst was compared with some of reported catalytic systems in the reduction of nitrobenzenes (Table 3). The results showed that although the previously reported catalytic systems have good activity for reduction of nitrobenzenes; however, in most cases the reaction is performed in organic solvents at temperatures higher than that employed for the present catalyst. Also we used lower amount of catalyst (0.5 mol%) than previous reports. Moreover, the recycling times of the present Fe_3O_4@BOS@SB/In nanocatalyst were shown to be more or less superior than the most of previous catalysts.

Table 3. Comparative study of the efficiency of the Fe_3O_4@BOS@SB/In nanocatalyst with previously reported catalytic systems in the reduction of nitrobenzenes

Catalyst	Conditions	Time (min)	Recovery times	Ref.
[NAP-Mg-Pd (0)]	1.48 mol% catalyst, THF, r.t., H_2	120	5	[66]
Cu NPs	10 mol% catalyst, THF/H_2O, 50 °C, $NaBH_4$	120	3	[67]
AgNPs@CeO_2	25 mg catalyst, dodecane, 110 °C, H_2	360	2	[68]
Fe_3O_4@PDA–Au	0.2 mg catalyst, water, r.t., $NaBH_4$	7-120	8	[69]
Co-L1/C	1 mol% catalyst, THF/H_2O, 110 °C, H_2	360	10	[70]
Pd/PEG	100 mg catalyst, EtOH, r.t., H_2	180	10	[71]
$In_2(OH)_3(BDC)_{1.5}$	5 mol% catalyst, 40 °C (autoclave), H_2	220	4	[72]
Fe_3O_4@BOS@SB/In	0.5 mol% catalyst, water, r.t., $NaBH_4$	12	6	This work

Abbreviations: [NAP-Mg-Pd (0)]: Nanocrystalline magnesium oxide-stabilized palladium (0). AgNPs@CeO_2: Silver–Cerium dioxide core–shell nanocomposite. Fe_3O_4@PDA–Au: gold nanoparticles on the surface of polydopamine (PDA)-encapsulated Fe_3O_4 nanoparticles. Co-L1/C: cobalt oxide-phenanthrolinev/carbon. Pd/PEG: palladium nanoparticles in polyethylene glycol (PEG). BDC: 1,4-benzendicarboxylate

It is also important to note that using hydrogen gas in reduction is so dangerous, because of explosion potential, but in this report we used sodium borohydride that is safe, affordable and has a mild reaction condition. These findings significantly confirm the high efficiency of the present catalyst in the reduction of different derivatives of nitrobenzenes.

4. Conclusion

In conclusion, for the first time a novel magnetic bifunctional organosilica supported indium/Schiff-base catalyst (Fe_3O_4@BOS@SB/In) was prepared. The magnetic properties of this were investigated using VSM showing good magnetic ability of the material. TG analysis confirmed well immobilization of ethyl and propyl-Schiff-base functional groups on magnetic iron oxide cores and also showed high thermal stability of the catalyst. Energy-dispersive X-ray spectroscopy (EDS) demonstrated the presence of expected In, Fe, Si, C, N, O and Cl elements in the material. Also the FT-IR analysis confirmed the EDS and TGA results and successfully proved the presence of expected functional groups in the structure of the material. The morphology and particle size of the catalyst was determined using SEM and TEM analyses. These demonstrated a core-shell structure with spherical morphology for the catalyst. The PXRD pattern confirmed the high stability of Fe_3O_4 NPs during catalyst preparation. The catalytic efficiency of the designed Fe_3O_4@BOS@SB/In nanocatalyst was studied in the reduction of nitrobenzene in which some parameters such as temperature, catalyst loading and solvent were optimized. A set of different nitrobenzene derivatives were converted to their corresponding anilines in the presence of low loading of catalyst. The designed Fe_3O_4@BOS@SB/In was also recovered and reused at least 6 times with keeping its performance. The leaching test and PXRD analysis of the recovered catalyst showed high stability and durability of this material during

applied conditions. Other advantages of the present study are the use of water as solvent, easy product and catalyst separation and high reaction rate at green conditions. Some applications of this catalyst in other organic transformations are underway in our laboratories.

References

[1] J. Belleson, E. Grochowski, The era of giant magnetoresistive heads, Hitachi Global Storage Technologies, (1998).

[2] M. Kanellos, A Divide Over the Future of Hard Drives, Cnet News, published Aug, 23 (2006).

[3] H.V. Thakur, S.M. Nalawade, S. Gupta, R. Kitture, S. Kale, Photonic crystal fiber injected with Fe3O4 nanofluid for magnetic field detection, ApPhL, 99 (2011) 161101.

[4] C. Ban, Z. Wu, D.T. Gillaspie, L. Chen, Y. Yan, J.L. Blackburn, A.C. Dillon, Nanostructured Fe3O4/swnt electrode: binder□free and high□rate li□ion anode, Adv. Mater., 22 (2010).

[5] S. Abanades, I. Villafan□Vidales, CO2 valorisation based on Fe3O4/FeO thermochemical redox reactions using concentrated solar energy, Int. J. Energy Res., 37 (2013) 598-608.

[6] S.-W. Cao, Y.-J. Zhu, M.-Y. Ma, L. Li, L. Zhang, Hierarchically nanostructured magnetic hollow spheres of Fe3O4 and γ-Fe2O3: preparation and potential application in drug delivery, J. Phys. Chem. C, 112 (2008) 1851-1856.

[7] Y. Zhu, T. Ikoma, N. Hanagata, S. Kaskel, Rattle□type Fe3O4@ SiO2 hollow mesoporous spheres as carriers for drug delivery, Small, 6 (2010) 471-478.

[8] X. Li, X. Huang, D. Liu, X. Wang, S. Song, L. Zhou, H. Zhang, Synthesis of 3D hierarchical Fe3O4/graphene composites with high lithium storage capacity and for controlled drug delivery, J. Phys. Chem. C, 115 (2011) 21567-21573.

[9] F. Chen, Q. Gao, J. Ni, The grafting and release behavior of doxorubincin from Fe3O4@ SiO2 core–shell structure nanoparticles via an acid cleaving amide bond: the potential for magnetic targeting drug delivery, Nanotechnology, 19 (2008) 165103.

[10] Y. Zhu, Y. Fang, S. Kaskel, Folate-conjugated Fe3O4@ SiO2 hollow mesoporous spheres for targeted anticancer drug delivery, J. Phys. Chem. C, 114 (2010) 16382-16388.

[11] Z. Yuanbi, Q. Zumin, J. Huang, Preparation and Analysis of Fe3O4 Magnetic Nanoparticles Used as Targeted-drug Carriers Supported by the Technology Project of Jiangxi Provincial Education Department and Jiangxi Provincial Science Department, Chin. J. Chem. Eng., 16 (2008) 451-455.

[12] X. Wang, R. Zhang, C. Wu, Y. Dai, M. Song, S. Gutmann, F. Gao, G. Lv, J. Li, X. Li, The application of Fe3O4 nanoparticles in cancer research: a new strategy to inhibit drug resistance, J Biomed Mater Res A, 80 (2007) 852-860.

[13] B.-L. Lin, X.-D. Shen, S. Cui, Application of nanosized Fe3O4 in anticancer drug carriers with target-orientation and sustained-release properties, Biomed. Mater., 2 (2007) 132.

[14] D. Pan, H. Zhang, T. Fan, J. Chen, X. Duan, Nearly monodispersed core–shell structural Fe3O4@ DFUR–LDH submicro particles for magnetically controlled drug delivery and release, Chem. Commun., 47 (2011) 908-910.

[15] X. Lou, J. Huang, T. Li, H. Hu, B. Hu, Y. Zhang, Hydrothermal synthesis of Fe3O4 and α-Fe2O3 nanocrystals as anode electrode materials for rechargeable Li-ion batteries, J. Mater. Sci.: Mater. Electron., 25 (2014) 1193-1196.

[16] T.A. Gad-Allah, S. Kato, S. Satokawa, T. Kojima, Treatment of synthetic dyes wastewater utilizing a magnetically separable photocatalyst (TiO2/SiO2/Fe3O4): Parametric and kinetic studies, Desalination, 244 (2009) 1-11.

[17] Y. Jiao, D. Han, L. Liu, L. Ji, G. Guo, J. Hu, D. Yang, A. Dong, Highly Ordered Mesoporous Few□Layer Graphene Frameworks Enabled by Fe3O4 Nanocrystal Superlattices, Angew. Chem., 127 (2015) 5819-5823.

[18] W. Gu, X. Deng, X. Gu, X. Jia, B. Lou, X. Zhang, J. Li, E. Wang, Stabilized, superparamagnetic functionalized graphene/Fe3O4@ Au nanocomposites for a magnetically-controlled solid-state electrochemiluminescence biosensing application, AnaCh, 87 (2015) 1876-1881.

[19] H. Veisi, A. Sedrpoushan, B. Maleki, M. Hekmati, M. Heidari, S. Hemmati, Palladium immobilized on amidoxime functionalized magnetic Fe3O4 nanoparticles: a highly stable and efficient magnetically recoverable nanocatalyst for sonogashira coupling reaction, Appl Organomet Chem, 29 (2015) 834-839.

[20] N. Zohreh, S.H. Hosseini, A. Pourjavadi, C. Bennett, Immobilized copper (II) on nitrogen rich polymer entrapped Fe3O4 nanoparticles: a highly loaded and magnetically recoverable catalyst for aqueous click chemistry, Appl Organomet Chem, 30 (2016) 73-80.

[21] S. Wang, Z. Zhang, B. Liu, Catalytic Conversion of Fructose and 5-Hydroxymethylfurfural into 2, 5-Furandicarboxylic Acid over a Recyclable Fe3O4–CoO x Magnetite Nanocatalyst, ACS SUSTAIN. CHEM. ENG, 3 (2015) 406-412.

[22] L. Z Fekri, M. Nikpassand, K. H Pour, Green aqueous synthesis of mono, bis and trisdihydropyridines using nano Fe3O4 under ultrasound irradiation, Curr. Org. Synth., 12 (2015) 76-79.

[23] M.A. Tamilmagan, G.A. PriyaBijesh, Biodiesel production from waste cooking oil using green synthesized nanoFe2O3 and CuO impregnated nano Fe3O4, Int J Chemtech Res, 8 (2015) 90-96.

[24] K. Osouli-Bostanabad, H. Aghajani, E. Hosseinzade, H. Maleki-Ghaleh, M. Shakeri, High microwave absorption of nano-Fe3O4 deposited electrophoretically on carbon fiber, MMP, 31 (2016) 1351-1356.

[25] B. Amirheidari, M. Seifi, M. Abaszadeh, Evaluation of magnetically recyclable nano-Fe3O4 as a green catalyst for the synthesis of mono-and bis-tetrahydro-4H-chromene and mono and bis 1, 4-dihydropyridine derivatives, Res. Chem. Intermed., 42 (2016) 3413-3423.

[26] A.R. Kiasat, M. Daei, S.J. Saghanezhad, Synthesis and characterization of a novel nano-Fe3O4-copoly [(styrene/acrylic acid)/grafted ethylene oxide and its application as a magnetic and recyclable phase-transfer catalyst in the preparation of β-azido alcohols and β-nitro alcohols, Res. Chem. Intermed., 42 (2016) 581-594.

[27] T. Wu, Y. Liu, X. Zeng, T. Cui, Y. Zhao, Y. Li, G. Tong, Facile hydrothermal synthesis of Fe3O4/C core–shell nanorings for efficient low-frequency microwave absorption, ACS Appl. Mater. Interfaces, 8 (2016) 7370-7380.

[28] A. Samadi, M. Amjadi, Magnetic Fe3O4@ C nanoparticles modified with 1-(2-thiazolylazo)-2-naphthol as a novel solid-phase extraction sorbent for preconcentration of copper (II), Microchim. Acta, 182 (2015) 257-264.

[29] X. Wang, B. Song, M. Huo, Y. Song, Z. Lv, Y. Zhang, Y. Wang, Y. Song, J. Wen, Y. Sui, Fast and sensitive lateral photovoltaic effects in Fe3O4/Si Schottky junction, RSC Adv., 5 (2015) 65048-65051.

[30] K. Faghihi, A. Raeisi, M. Amini, M. Shabanian, A.R. Karimi, Sulfonic acid-functionalized Fe3O4 reinforced soluble polyimide: synthesis and properties, Polym.-Plast. Technol. Eng., 55 (2016) 259-267.

[31] T. Wang, L. Zhang, C. Li, W. Yang, T. Song, C. Tang, Y. Meng, S. Dai, H. Wang, L. Chai, Synthesis of core–shell magnetic Fe3O4@ poly (m-phenylenediamine) particles for chromium reduction and adsorption, Environ Sci Technol, 49 (2015) 5654-5662.

[32] Y. Chen, J. Nan, Y. Lu, C. Wang, F. Chu, Z. Gu, Hybrid Fe3O4-poly (acrylic acid) Nanogels for theranostic cancer treatment, J. Biomed. Nanotechnol., 11 (2015) 771-779.
[33] X. Liu, X. Zhao, M. Lu, Pd Nanoparticles Immobilized on Fe3O4@ Poly (ethylene glycol) Bridged Amine Functionalized Imidazolium Ionic Liquid: A Magnetically Separable Catalyst for Heck in Water, CatL, 145 (2015) 1549-1556.
[34] Y. Jiang, J. Jiang, Q. Gao, M. Ruan, H. Yu, L. Qi, A novel nanoscale catalyst system composed of nanosized Pd catalysts immobilized on Fe3O4@ SiO2–PAMAM, Nanotechnology, 19 (2008) 075714.
[35] L. Zhou, C. Gao, W. Xu, Robust Fe3O4/SiO2-Pt/Au/Pd magnetic nanocatalysts with multifunctional hyperbranched polyglycerol amplifiers, Langmuir, 26 (2010) 11217-11225.
[36] M. Shao, F. Ning, J. Zhao, M. Wei, D.G. Evans, X. Duan, Preparation of Fe3O4@ SiO2@ layered double hydroxide core–shell microspheres for magnetic separation of proteins, J. Am. Chem. Soc., 134 (2012) 1071-1077.
[37] D. Elhamifar, P. Mofatehnia, M. Faal, Magnetic Nanoparticles Supported Schiff-base/Copper Complex: An Efficient Nanocatalyst for Preparation of Biologically Active 3, 4-Dihydropyrimidinones, J. Colloid Interface Sci., (2017).
[38] M. Ma, F. Yan, M. Yao, Z. Wei, D. Zhou, H. Yao, H. Zheng, H. Chen, J. Shi, Template-Free Synthesis of Hollow/Porous Organosilica–Fe3O4 Hybrid Nanocapsules toward Magnetic Resonance Imaging-Guided High-Intensity Focused Ultrasound Therapy, ACS Appl. Mater. Interfaces, 8 (2016) 29986-29996.
[39] J. Li, Y. Wei, W. Li, Y. Deng, D. Zhao, Magnetic spherical cores partly coated with periodic mesoporous organosilica single crystals, Nanoscale, 4 (2012) 1647-1651.
[40] H. Yang, G. Li, Z. Ma, Magnetic core–shell-structured nanoporous organosilica microspheres for the Suzuki–Miyaura coupling of aryl chlorides: improved catalytic activity and facile catalyst recovery, J. Mater. Chem., 22 (2012) 6639-6648.
[41] Z. Yacob, A. Nan, J. Liebscher, Proline□Functionalized Magnetic Core□Shell Nanoparticles as Efficient and Recyclable Organocatalysts for Aldol Reactions, Adv. Synth. Catal., 354 (2012) 3259-3264.
[42] P. Bhanja, T. Sen, A.J.J.o.M.C.A.C. Bhaumik, A magnetically recoverable nanocatalyst based on functionalized mesoporous silica, J. Mol. Catal. A: Chem., 415 (2016) 17-26.
[43] J. Mondal, T. Sen, A.J.D.T. Bhaumik, Fe3O4@ mesoporous SBA-15: a robust and magnetically recoverable catalyst for one-pot synthesis of 3, 4-dihydropyrimidin-2 (1 H)-ones via the Biginelli reaction, Dalton Trans., 41 (2012) 6173-6181.
[44] M. Hasanzadeh, F. Farajbakhsh, N. Shadjou, A. Jouyban, Mesoporous (organo) silica decorated with magnetic nanoparticles as a reusable nanoadsorbent for arsenic removal from water samples, Environ Technol, 36 (2015) 36-44.
[45] J. Kim, H.S. Kim, N. Lee, T. Kim, H. Kim, T. Yu, I.C. Song, W.K. Moon, T. Hyeon, Multifunctional uniform nanoparticles composed of a magnetite nanocrystal core and a mesoporous silica shell for magnetic resonance and fluorescence imaging and for drug delivery, Angew. Chem. Int. Ed., 47 (2008) 8438-8441.
[46] A.K. Gupta, M. Gupta, Cytotoxicity suppression and cellular uptake enhancement of surface modified magnetic nanoparticles, Biomaterials, 26 (2005) 1565-1573.
[47] T. Mahmood, A. Elliott, A review of secondary sludge reduction technologies for the pulp and paper industry, Water Res, 40 (2006) 2093-2112.

[48] D.J. Constable, P.J. Dunn, J.D. Hayler, G.R. Humphrey, J.L. Leazer Jr, R.J. Linderman, K. Lorenz, J. Manley, B.A. Pearlman, A. Wells, Key green chemistry research areas—a perspective from pharmaceutical manufacturers, Green Chem., 9 (2007) 411-420.
[49] Z. Szcygiel, C. Lara, S. Escobedo, O. Mendoza, The direct reduction of sulfide minerals for the recovery of precious metals, JOM, 50 (1998) 55.
[50] A. Pielesz, The process of the reduction of azo dyes used in dyeing textiles on the basis of infrared spectroscopy analysis, J. Mol. Struct., 511 (1999) 337-344.
[51] D. Hartter, The Use and Importance, Toxicity of nitroaromatic compounds, 1 (1985).
[52] L.-X. Cheng, J.-J. Tang, H. Luo, X.-L. Jin, F. Dai, J. Yang, Y.-P. Qian, X.-Z. Li, B. Zhou, Antioxidant and antiproliferative activities of hydroxyl-substituted Schiff bases, Bioorg. Med. Chem. Lett., 20 (2010) 2417-2420.
[53] U. Sharma, P.K. Verma, N. Kumar, V. Kumar, M. Bala, B. Singh, Phosphane□Free Green Protocol for Selective Nitro Reduction with an Iron□Based Catalyst, Chem. Eur. J., 17 (2011) 5903-5907.
[54] A. Corma, P. Serna, Chemoselective hydrogenation of nitro compounds with supported gold catalysts, Sci, 313 (2006) 332-334.
[55] N. Pradhan, A. Pal, T. Pal, Silver nanoparticle catalyzed reduction of aromatic nitro compounds, Colloids Surf. Physicochem. Eng. Aspects, 196 (2002) 247-257.
[56] E. Yilmaz, M.J.J.o.t.I.C.S. Soylak, Facile and green solvothermal synthesis of palladium nanoparticle-nanodiamond-graphene oxide material with improved bifunctional catalytic properties, 14 (2017) 2503-2512.
[57] E. Yilmaz, Y. Tut, O. Turkoglu, M.J.J.o.t.I.C.S. Soylak, Synthesis and characterization of Pd nanoparticle-modified magnetic Sm 2 O 3–ZrO 2 as effective multifunctional catalyst for reduction of 2-nitrophenol and degradation of organic dyes, 15 (2018) 1721-1731.
[58] S.K. Ghosh, M. Mandal, S. Kundu, S. Nath, T. Pal, Bimetallic Pt–Ni nanoparticles can catalyze reduction of aromatic nitro compounds by sodium borohydride in aqueous solution, Appl. Catal., A, 268 (2004) 61-66.
[59] C.J. Moody, M.R. Pitts, Indium as a reducing agent: reduction of aromatic nitro groups, Synlett, 1998 (1998) 1028-1028.
[60] J.Z. Saavedra, A. Resendez, A. Rovira, S. Eagon, D. Haddenham, B. Singaram, Reaction of InCl3 with various reducing agents: InCl3–NaBH4-mediated reduction of aromatic and aliphatic nitriles to primary amines, J. Org. Chem., 77 (2011) 221-228.
[61] Y.S. Kang, S. Risbud, J.F. Rabolt, P. Stroeve, Synthesis and characterization of nanometer-size Fe3O4 and γ-Fe2O3 particles, Chem. Mater., 8 (1996) 2209-2211.
[62] D.C. Barman, A.J. Thakur, D. Prajapati, J.S. Sandhu, InCl3-Zn. A Novel Reduction System for the Deoxygenative Coupling of Carbonyl Compounds to Olefins, Synlett, 2001 (2001) 0515-0516.
[63] P. Li, L. Wang, Y. Yang, X. Sun, M. Wang, J. Yan, A novel reduction of sodium alkyl thiosulfates with InCl3 (cat.)/Sm (0) system in aqueous media: Facile synthesis of disulfides, Heteroat. Chem, 15 (2004) 376-379.
[64] A. E Johnson, V. Tamara Perchyonok, On the Scope of Radical Reactions Utilizing InCl3/coreductant as an Efficient Reagent for Synthetically Useful Transformations in Aqueous and Organic Solvents, Curr. Org. Chem., 14 (2010) 2007-2011.
[65] Aldrich Catalog Handbook of Fine Chemicals, in: A.C. Company (Ed.), 2012–2014.

[66] M.L. Kantam, R. Chakravarti, U. Pal, B. Sreedhar, S. Bhargava, Nanocrystalline Magnesium Oxide Stabilized Palladium (0): An Efficient and Reusable Catalyst for Selective Reduction of Nitro Compounds, Adv. Synth. Catal., 350 (2008) 822-827.
[67] Z. Duan, G. Ma, W. Zhang, Preparation of copper nanoparticles and catalytic properties for the reduction of aromatic nitro compounds, Bull. Korean Chem. Soc., 33 (2012) 4003-4006.
[68] T. Mitsudome, Y. Mikami, M. Matoba, T. Mizugaki, K. Jitsukawa, K. Kaneda, Design of a silver–cerium dioxide core–shell nanocomposite catalyst for chemoselective reduction reactions, Angew. Chem. Int. Ed., 51 (2012) 136-139.
[69] T. Zeng, H.-y. Niu, Y.-r. Ma, W.-h. Li, Y.-q. Cai, In situ growth of gold nanoparticles onto polydopamine-encapsulated magnetic microspheres for catalytic reduction of nitrobenzene, Appl. Catal., B, 134 (2013) 26-33.
[70] F.A. Westerhaus, R.V. Jagadeesh, G. Wienhöfer, M.-M. Pohl, J. Radnik, A.-E. Surkus, J. Rabeah, K. Junge, H. Junge, M. Nielsen, Heterogenized cobalt oxide catalysts for nitroarene reduction by pyrolysis of molecularly defined complexes, Nat. Chem., 5 (2013) 537-543.
[71] F. Harraz, S. El-Hout, H. Killa, I. Ibrahim, Palladium nanoparticles stabilized by polyethylene glycol: Efficient, recyclable catalyst for hydrogenation of styrene and nitrobenzene, J. Catal., 286 (2012) 184-192.
[72] B. Gomez-Lor, E. Gutierrez-Puebla, M. Iglesias, M. Monge, C. Ruiz-Valero, N. Snejko, In2 (oh) 3 (bdc) 1.5 (bdc= 1, 4-benzendicarboxylate): an In (iii) supramolecular 3d framework with catalytic activity, Inorg. Chem., 41 (2002) 2429-2432.

Highlights

1. A novel magnetic bifunctional organosilica with core-shell structure supported indium (Fe_3O_4@BOS@SB/In) was prepared
2. The Fe_3O_4@BOS@SB/In was characterized using SEM, TGA, VSM, FT-IR, EDX and PXRD
3. This was applied as a powerful and heterogeneous nanocatalyst in the reduction of nitrobenzenes
4. The recoverability, reusability and durability of the catalyst have also been studied